Real-time measurement of track irregularities using an instrumented axle and Kalman filtering techniques

Sergio Munoz
Department of Materials and Transportation Engineering
Escuela Técnica Superior de Ingeniería
University of Seville
Spain
Email: sergiomunoz@us.es

Pedro Urda
Department of Mechanical and Manufacturing Engineering
Escuela Técnica Superior de Ingeniería,
Escuela Politécnica Superior
University of Seville
Spain
Email: purda@us.es

Xinxin Yu
Department of Mechanical and Manufacturing Engineering
Escuela Técnica Superior de Ingeniería
University of Seville
Spain
Email: yxinxin@us.es

Aki Mikkola
Department of Mechanical Engineering
Lappeenranta University of Technology
Finland
Email: Aki.Mikkola@lut.fi

Jose Luis Escalona
Department of Mechanical and Manufacturing Engineering
Escuela Técnica Superior de Ingeniería
University of Seville
Spain
Email: escalona@us.es

ABSTRACT

A model-based methodology for the estimation of both lateral and vertical track irregularities is presented. This methodology, based on Kalman filter techniques, was developed for an independent and compact measuring system comprising an instrumented axle equipped with a limited set of low-cost sensors: a 3D gyroscope, a Linear Variable Differential Transformer (LVDT) distance sensor and an encoder. The instrumented axle can be used on any railway vehicle travelling at moderate forward speed to provide measurements in real-time. The proposed methodology, combined with the instrumented axle, enables precise and prompt measurement of track irregularities.

An experimental campaign carried out on a 1:10 scale track facility at the University of Seville validated both the system and the methodology. In the testing, 80 meters of scaled track was measured at an operational speed of V = 0.65 m/s in just two minutes. Simulation estimates for track irregularities compared against the measured data from the testing showed a good performance of the proposed methodology, with maximum errors of 0.45 mm in the short wavelength range D1, the range most influential to vehicle dynamic behavior.

1 Introduction

The growth of rail traffic and the increase in the speed of vehicles is a major burden on the track system, which suffers significant deterioration. Consequently, track irregularity measurements are critical to ensuring the safety and reliability of railway transportation. These measurements allow for early detection of track defects and can help rail operators optimize their maintenance schedules to minimize downtime and reduce costs. In European countries, track irregularities are regulated by the EN13848 Standard [1], which defines the limit levels for irregularity amplitude as a function of their wavelength in three different ranges: $D_1 = [3, 25]$ m , $D_2 = [25, 70]$ m and $D_3 = [70, 200]$ m. Consequently, track geometry must be analyzed

according to the different irregularity wavelength ranges defined in the standard. In the railway industry, track maintenance mainly depends on a continuous monitoring of track geometry, which can be carried out using a variety of methods.

The traditional way to survey track geometry is to use measuring trolleys, which are normally pushed by a human operator. These trolleys are equipped with a set of sensors to measure relative irregularities: encoder, distance sensor and inclinometer. In addition, a method to determine absolute positioning on the track is needed. Absolute position can be established using a total station, which allows a precise but non-continuous ("stop and go") measurement of the track [2]. An considerable improvement is the use of Global Navigation Satellite System/Inertial Navigation System (GNSS/INS) systems in track geometry measurements, which allows continuous measurement with acceptable precision [3]. However, the main weakness of these methods is reduced measurement speed (around 100 meters per hour).

Lately, the most widespread track measurement method is to use special Track recording vehicles (TRV) that accurately measure track geometry using different sets of sensors (optical, laser distance or inertial sensors) [4]. The main inconvenience of TRVs is their complexity and high cost. The alternative to such a high-priced TRVs is inexpensive measuring systems mounted on in-service vehicles for continuous monitoring of track conditions. This methodology is mainly based on a simple measuring system, combined with a dynamic model-based method [5, 6]. However, estimating track irregularities from vehicle dynamic behavior is difficult, because it is governed by highly non-linear equations. Several research works have been published in recent years analysing the best measuring system to be adopted in in-service vehicles for track condition monitoring [7]. The position of the sensors in the vehicle is crucial and is strictly dependent on the type of irregularities to be identified: to detect short wavelength irregularities, the sensors should be placed very close to the wheel-rail system. Otherwise, the high frequencies can be filtered out by the primary suspension. Consequently, sensors mounted on the axlebox are used to detect short wavelenght irregularities, such as rail corrugation, while sensors mounted on the bogie frame are commonly used to detect long wavelength irregularities. The simplest way to monitor track irregularities is to integrate different signals, such as accelerometer or gyroscope, to obtain track geometry. This methodology was used by different authors to estimate short wavelength track irregularities from accelerometers mounted on the axlebox [8]. Analogously, other authors have used this methodology to estimate long wavelengths irregularities from sensors mounted on the bogie-frame, such as accelerometers [9, 10] or gyroscopes [11, 12].

A more sophisticated way of estimating track irregularities is to combine dynamics model-based methods with Kalman filtering techniques. Some authors have used the Kalman filter technique as a kind of integrator to predict track irregularities from vehicle acceleration. In [13], Tsunashima *et al.* measured vertical track irregularities from car -body's acceleration, while in [14], Lee *et al.* measured both vertical and lateral irregularities from accelerations in the axle box and bogie frame. More recently, De Rosa *et al.* [15] presented different approaches to estimate lateral irregularities based on vehicle dynamics measurements using a complex linear dynamic model of a railway vehicle, obtaining promising results. In [16], Munoz *et al.* proposed a model-based methodology for the estimation of lateral track irregularities from measurements from sensors mounted on an in-service vehicle. This methodology was experimentally validated, obtaining a very good performance.

A booming area that is receiving a significant attention is the use of machine learning algorithms for the measurement of track irregularities, including probabilistic methods, Artificial Neural Network (ANN) and Support Vector Machine (SVM). A complete review on this topic can be found in [17]. The main disadvantage of machine learning algorithms is that, being mainly based on the use of a large amount of data, its performance strongly depends on the quality of this data. Another weakness is that machine learning algorithms are not based on physical models, making it more difficult to interpret the data or identify sources of errors.

As a consequence of all the above, Kalman filtering method can be considered one of the most scientific and reliable approaches for track irregularity estimation. It offers excellent performance with real-time capabilities. The authors [18] proposed an model-based Kalman filter procedure for the estimation of both lateral and vertical track irregularities from the signals of different sensors mounted on a dedicated rail vehicle. This method was experimentally validated with good results for a scaled vehicle and track. The method was only based on measurement from inertial sensors installed on the vehicle. A total station, optical sensors, lasers, and video recording were not needed. It enabled fast and accurate measurement of track irregularities. Furthermore, since the method is based exclusively on a simple kinematic model of the vehicle, it offers excellent performance.

Based on the previous work [18], the authors here propose a new modified methodology for measuring track irregularities with three improvements to highlight. Firstly, instead of using a complete Track recording vehicle, it uses only an instrumented axle, which makes the measuring system more easily implemented in an actual real-world scenario. Consequently, with the new reduced configuration of the measurement system, the instrumented axle must be driven somehow and the most plausible way is by any real vehicle used in the railway industry: a passenger train, a freight train, a small bogie vehicle, etc. From the practical point of view, this represents a significant improvement, since the preparation time of the measurement system is significantly reduced before the measurement process. The instrumented axle is pre-calibrated and tuned in the laboratory, so it takes just few minutes to connect to the vehicle before the track measurement process. Secondly, it uses an improved Kalman filter, developed for this methodology, that makes use of a limited set of sensors: a 3D gyroscope, a Linear Variable Differential Transformer (LVDT) distance sensor, and an encoder. Accelerometers are no longer needed in the present methodology. This is also a major improvement, due to the inherent difficulty of using accelerome-

ters. Accelerometers provide a very noisy signal which requires a complex signal processing to extract useful information from them. Thirdly, the Kalman filter algorithm being used was programmed in the C language and implemented in the acquisition system, which makes the proposed procedure real-time capable. This improvement is quite relevant, as it enables the measurement system to provide a direct measurement of track irregularities in real time, without any type of subsequent post-processing. Compared with the existing methodologies that are implemented in the railways industry, the proposed measuring system brings several advances to the railways industry, from the scientific and the practical point of view: it is based on a very reduced and non-expensive set of sensors and on a kinematic model based Kalman filter, which is able to work in real time. Furthermore, the measuring system has been reduced to the minimum: a very compact instrumented axle, affordable for any railways maintenance operator. All this makes the proposed measuring system a serious alternative to other expensive and time-consuming methods for measuring track geometry.

The organization of this paper is as follows: Section 2 presents the usual definition of track irregularities in the railway industry. Section 3 describes the kinematics of the irregular track and the instrumented axle used in the present work. Section 4 explains, in detail, the proposed estimation technique. The experimental campaign used to validate the proposed methodology is described in Section 5. The results obtained in the estimation of track irregularities are presented in Section 6, along with their corresponding analysis in the different wavelength ranges according to the standard. Finally, the main conclusions are summarized in Section 7.

2 Description of track geometry

Track geometry is the superposition of the design geometry and the irregularities, see Fig. 1.

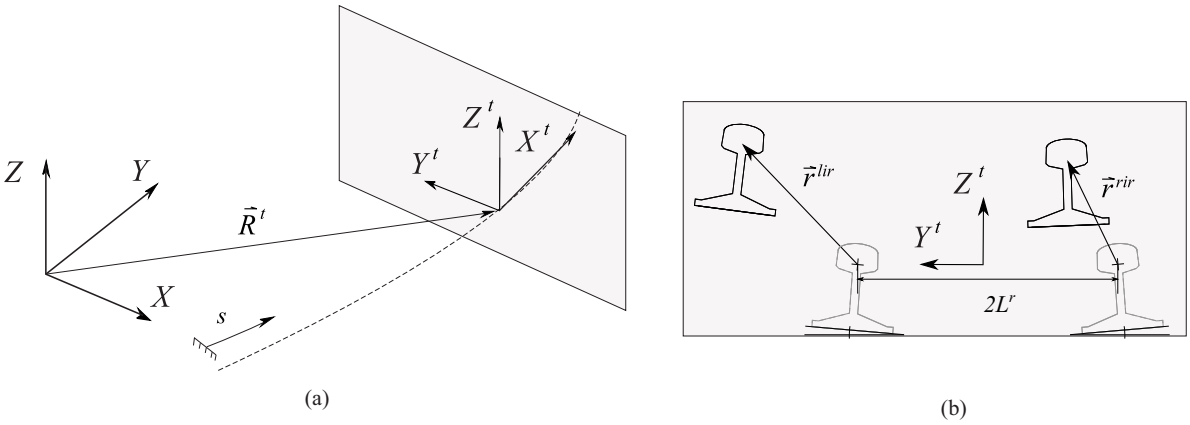

Fig. 1. Description of track geometry: (a) Position of the TF, (b) Irregularities in the $(Y^t - Z^t)$ plane

The design geometry is defined by the position of the track centerline, through the *Track frame* (TF) $< X^t, Y^t, Z^t >$, which is function of arc-length coordinate s. Consequently, as shown by in Fig.1 (a), the components of the absolute position vector of the TF with respect to an inertial and global frame (GF), $< X, Y, Z >$, is a function of arc-length s, as follows.

$$\mathbf{R}^t(s) = \begin{bmatrix} R_x^t(s) \\ R_y^t(s) \\ R_z^t(s) \end{bmatrix} \tag{1}$$

The orientation of the *Track frame* with respect to the GF can be measured with the Euler angles: ψ^t (heading angle), θ^t (vertical slope) and φ^t (cant angle). Even though the heading angle ψ^t can have an arbitrary value, the other two angles (θ^t and φ^t) can be considered small. With this assumption, the small angle approximation of the rotation matrix from the TF to the GF is given:

$$\mathbf{A}^t(s) \simeq \begin{bmatrix} \cos\psi^t & -\sin\psi^t & \varphi^t\sin\psi^t + \theta^t\cos\psi^t \\ \sin\psi^t & \cos\psi^t & \theta^t\sin\psi^t - \varphi^t\cos\psi^t \\ -\theta^t & \varphi^t & 1 \end{bmatrix} \tag{2}$$

The accuracy of this assumption can be easily tested by using the usual values of both angles (θ^t and φ^t) in the design geometry of tracks, known in the railways industry: both angles are always less than 5º, which leads to errors less than 0.1%.

At each track section, the track centerline geometry can be defined by the following geometric variables: twist curvature ρ_{tw}, vertical curvature ρ_v and horizontal curvature ρ_h. These variables can be calculated as the space derivatives of φ^t, θ^t and ψ^t with respect to the arc-length s, respectively.

Track irregularities can be defined as the deviation of the rail heads with respect to their design position, in the track cross section ($Y^t - Z^t$ plane), as it can be seen in Fig.1 (b). Consequently, track irregularities are given by two different irregularity vectors, corresponding to both left ($\vec{r}^{lir}$) and right ($\vec{r}^{rir}$) rails. Both vectors are defined in the *Track frame*, as a function of arc-length s:

$$\bar{\mathbf{r}}^{lir} = \begin{bmatrix} 0 \\ y^{lir} \\ z^{lir} \end{bmatrix}, \quad \bar{\mathbf{r}}^{rir} = \begin{bmatrix} 0 \\ y^{rir} \\ z^{rir} \end{bmatrix} \tag{3}$$

Finally, the following four combinations of rail head irregularities are measured.

$$\begin{array}{ll} \text{Alignment:} & \xi_{al} = \left(y^{lir} + y^{rir}\right)/2 \\ \text{Vertical profile:} & \xi_{vp} = \left(z^{lir} + z^{rir}\right)/2 \\ \text{Gauge variation:} & \xi_{gv} = y^{lir} - y^{rir} \\ \text{Cross level:} & \xi_{cl} = z^{lir} - z^{rir} \end{array} \tag{4}$$

Track irregularities can be classified in two different kinds: global and relative irregularities. Global irregularities (alignment and vertical profile) are the geometric deviation of the track centerline, while relative irregularities (gauge variation and cross-level) are the deviation of the relative position between both rails.

3 Kinematic model of the instrumented axle

3.1 Instrumented axle

One of the main improvement of the present methodology is the reduction of the measurement system: instead of using a complete Track recording vehicle, a reduced device consisting in a instrumented axle has been used. This instrumented axle has the advantage of being independent and easily connectable to any real railway vehicle in just few minutes. The design of the instrumented axle can be seen in Figure 2.

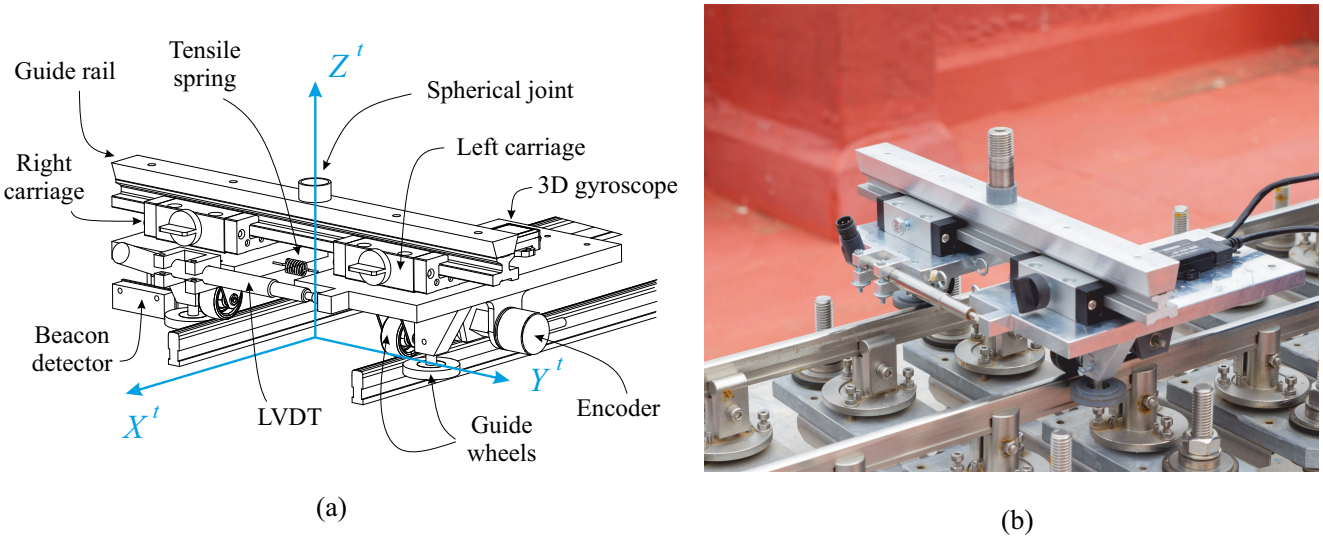

Fig. 2. Instrumented axle: (a) CAD design, (b) real prototype

The instrumented axle consists of two carriages that slide along a guide rail. To ensure accurate track geometry measurement, the instrumented axle must precisely follow the track's geometry. To accomplish this, lateral guide wheels are fitted on both sides of the instrumented axle, and a tensile spring connects the carriages. During measurement, the left carriage, which houses the 3D gyroscope, is locked in place, enabling the gyroscope to follow the left rail geometry. The right carriage is free to move along the guide rail, allowing for the direct measurement of track gauge variation using an LVDT attached to the carriage (see Fig. 2 (a)). The selection of the left carriage to house the gyroscope is totally arbitrary (it could be installed on the right carriage). Note that, the numerical procedure is based on the signals from the gyroscope. Regardless the exact position of the gyroscope, it is capable of measuring the curvatures of the track center-line: since the angular velocity of a rigid body is the same at any of its points, if the system is rigid, the gyroscope measures the same on the left rail or on the center-line.

Additionally, the instrumented axle has an odometry system that employs a precision encoder to measure the distance travelled while rolling without slipping. However, the distance measured by the encoder (installed in the left wheel) differs from the real arc-length coordinate s (defined in the track centre-line). This leads to an accumulative error of the arc-length s measured by the encoder. To correct this error, an odometry algorithm has been used in the present work: a beacon detector installed in the vehicle registers the position of magnetic beacons located along the track. Since the exact position of the beacons are known, the potential error in the arc-length coordinate is minimized. However, in a real case scenario in which there is no beacons distributed along the track, a different algorithm should be used. In [19], Escalona *et al.* developed an odometry algorithm for a railway vehicle, based on the curvatures of the track, whose theoretical values (from the design geometry of the track) are known a priori.

The kinematic model of the instrumented axle is presented in Fig. 3.

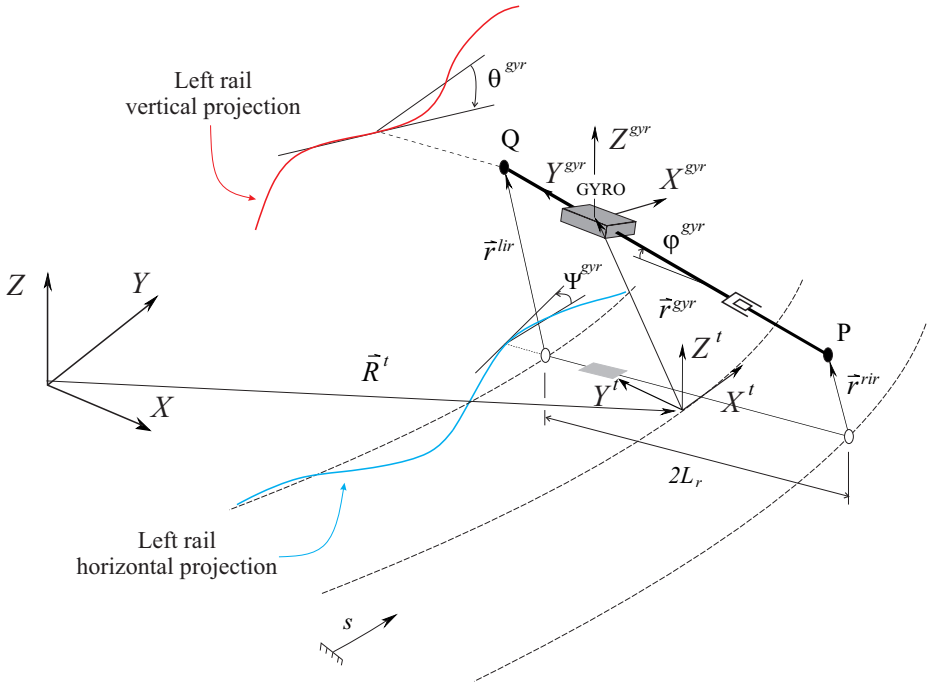

Fig. 3. Kinematics of the instrumented axle

This figure illustrates the movement of the *track frame* $< X^t, Y^t, Z^t >$ along the centerline of the track at a forward velocity V, with the irregularity vectors ($\vec{r}^{lir}$ and $\vec{r}^{rir}$) indicating the displacement of the rail centerlines from their design positions. The instrumented axle comprises two bodies, namely the left and right carriages in Fig. 2 (a), which are connected through a prismatic joint.

The following assumptions were taken into consideration.

1. The left body maintains contact with point Q on the centerline of the left rail, while the right body remains in contact with point P on the centerline of the right rail.
2. The axle connecting points Q and P is assumed to be perpendicular to the centerline of the left rail.
3. The gyroscope is installed in a vertical plane that contains points P and Q, with a constant distance with respect to point Q of d_y (lateral direction) and d_z (vertical direction).

4. The orientation of the gyroscope with respect to the TF is given by three Euler angles (φ^{gyr}, θ^{gyr} and ψ^{gyr}), which can be assumed to be small.

The first assumption is easily justified by the mechanical design of the apparatus, while the second assumption is more challenging to justify due to the non-parallel threads of the left and right rails. However, since the angle of the axle with respect to the perpendicular line is small, any resulting inaccuracies can be considered negligible. Although the third assumption is not exact, any inaccuracies are assumed to be small due to the proximity of the gyroscope to the line connecting points P and Q. In the last assumption, the relative angles of the gyroscope with respect to the TF are considered small, even on curved tracks, where the absolute angles may be significant. However, the relative angles always remain small in all cases, regardless of track curvature. These relative angles are typically on the order of milliradians, even smaller than the vertical slope (θ^t) and the cant angle (φ^t) of the track, resulting in even smaller errors due to linearization.

By utilizing the simplified assumptions established above, the kinematics of an irregular track depicted in Fig. 3 results in the following relationships.

$$\begin{aligned} r_y^{gyr} &= y^{lir} + L_r - d_y \\ r_z^{gyr} &= z^{lir} + d_z \\ \varphi^{gyr} &= (z^{lir} - z^{rir})/2L_r \\ \theta^{gyr} &= -\frac{dz^{lir}}{ds} = -z^{lir\prime} \\ \psi^{gyr} &= \frac{dy^{lir}}{ds} = y^{lir\prime} \\ d_{PQ} &= 2L_r + y^{lir} - y^{rir} \end{aligned} \tag{5}$$

where r_y^{gyr} and r_z^{gyr} are the non-zero components of the position vector of the gyroscope with respect to the TF, while $2L_r$ represents the nominal gauge, which is the distance between both rails in the absence of irregularities. The fourth and fifth expressions in Eq. 5 assume that the local axis X^{gyr} is consistently tangent to the 3D curve of the left rail, as indicated in the left rail's lateral and vertical projections in Fig. 3. The final expression assumes that the distance between points P and Q is equal to its horizontal projection.

Finally, the following expressions can be obtained by time-derivation of some expressions in Eqs. 5. These equalities will be useful later.

$$\begin{aligned} \dot{\varphi}^{gyr} &= V(z^{lir\prime} - z^{rir\prime})/2L_r \\ \dot{\theta}^{gyr} &= -V z^{lir\prime\prime} \\ \dot{\psi}^{gyr} &= V y^{lir\prime\prime} \end{aligned} \tag{6}$$

The angular velocities measured by the gyroscope here are the only inertial measurements included in the proposed methodology. The accelerations used in the previous work by the authors [18] are not required. That is the reason why accelerations have not been derived in Eq. 6.

3.2 Kinematics of the gyroscope

For the kinematic description of the gyroscope, the following coordinates are used.

$$\mathbf{q}^{gyr} = \left[s^{gyr} \; r_y^{gyr} \; r_z^{gyr} \; \varphi^{gyr} \; \theta^{gyr} \; \psi^{gyr} \right]^T \tag{7}$$

where s^{gyr} is the arc length of the track frame that follows the body motion, $\bar{\mathbf{r}}^i = \left[0 \; r_y^i \; r_z^i \right]^T$ is the local position vector of the gyroscope with respect to the TF resolved in the TF, and φ^{gyr}, θ^{gyr} and ψ^{gyr} are the three Euler angles that define the orientation of the gyroscope with respect to the TF. Out of the six coordinates used for the kinematic description of the gyroscope, only the arc-length coordinate s^{gyr} is an absolute coordinate. The other 5 are track-relative coordinates. The three Euler angles can be assumed to be small, which leads to the following kinematic linearization of the corresponding rotation matrix.

$$\mathbf{A}^{t,gyr} \simeq \begin{bmatrix} 1 & -\psi^{gyr} & \theta^{gyr} \\ \psi^{gyr} & 1 & -\varphi^{gyr} \\ -\theta^{gyr} & \varphi^{gyr} & 1 \end{bmatrix} \tag{8}$$

The absolute angular velocity of the gyroscope frame resolved in the gyroscope frame is given by [19]:

$$\hat{\omega}^{gyr} = \hat{\omega}^{t} + \hat{\omega}^{t,gyr} = \left(\mathbf{A}^{t,gyr}\right)^{T} \bar{\omega}^{t} + \hat{\omega}^{t,gyr} \tag{9}$$

In the previous equation, $\bar{\omega}^{t}$ is the absolute angular velocity of the TF, and $\hat{\omega}^{t,gyr}$ is the relative angular velocity of the gyroscope with respect to the TF resolved in the TF. Under the small-angles assumption, both expressions are given by:

$$\bar{\omega}^{t} = \begin{bmatrix} \rho_{tw} V \\ \rho_{v} V \\ \rho_{h} V \end{bmatrix} \tag{10}$$

$$\hat{\omega}^{t,gyr} = \begin{bmatrix} \dot{\varphi}^{gyr} \\ \dot{\theta}^{gyr} \\ \dot{\psi}^{gyr} \end{bmatrix} \tag{11}$$

Finally, the 3D gyroscope provides the measurement of the absolute angular velocity of the gyroscope in the sensor frame, as follows.

$$\omega^{gyr} = \hat{\omega}^{gyr} \tag{12}$$

where ω^{gyr} is an array that includes the quantities measured by the 3D gyroscope.

3.3 Simplifying assumptions

In order to simplify the preceding equations, the following assumptions were employed.

1. The roll and pitch angular velocities due to track design geometry can be considered negligible. This is equivalent to considering $\rho_{v} = \rho_{tw} = 0$.
2. The relative orientation of the gyroscope with respect to the TF is so small that the matrix $\mathbf{A}^{t,gyr}$ in Eq. 8 can be supposed to be the identity matrix.

After considering the simplifying assumptions, the signal obtained from the gyroscope, as presented in Equation 12, can be expressed as follows:

$$\omega^{gyr} = \begin{bmatrix} \omega_{x}^{gyr} \\ \omega_{y}^{gyr} \\ \omega_{z}^{gyr} \end{bmatrix} = \begin{bmatrix} \dot{\varphi}^{gyr} \\ \dot{\theta}^{gyr} \\ \dot{\psi}^{gyr} + \rho_{h} V \end{bmatrix} \tag{13}$$

The measurements used in the proposed methodology must be completed by the inclusion of the equation related to the gauge variation.

$$\xi_{gv}^{meas} = d_{PQ} - 2L_{r} = y^{lir} - y^{rir} \tag{14}$$

To obtain track gauge variation in Eq. 14, the nominal gauge ($2L_{r}$) must be subtracted from the measurement by the LVDT sensor d_{PQ}.

4 Irregularity estimation technique

4.1 Estimation procedure

The numeric procedure for the estimation of both lateral and vertical track irregularities is presented in this section. It represents an updated and improved methodology based on Kalman filtering techniques, previously presented by the authors in [18]. This is a fast and accurate methodology that, making use of different sensors mounted on an instrumented axle, provides the geometry of a track. One of the main improvements of the present methodology compared with the previous one is the elimination of the accelerometers. As previously mentioned, due to the inherent difficulty of using accelerometers with such noisy signals, their elimination from the measurement system represents an important advance. Consequently, the estimation procedure, which is based on the kinematic model of the instrumented axle presented in Section 3, is graphically defined in Fig. 4.

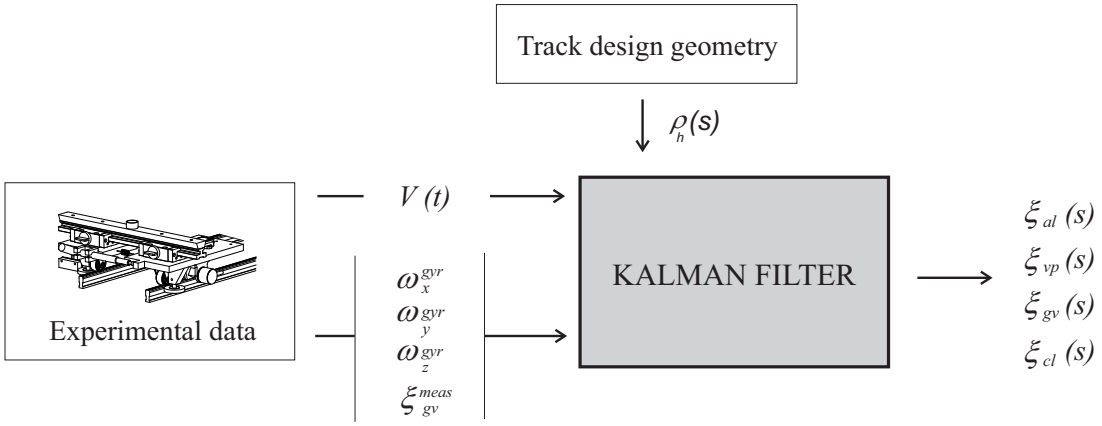

Fig. 4. Estimation technique

The Kalman filter has two different input types: the horizontal curvature of the design track centerline, (ρ_h), which is a function of arc-length coordinate s and the measurements obtained from the different sensors mounted in the instrumented axle, which are the vehicle forward velocity (V) from the odometry system, angular velocities (ω_x^{gyr}, ω_y^{gyr} and ω_z^{gyr}) from the gyroscope, and gauge variation (ξ_{gv}^{meas}) from the LVDT distance sensor. All these data from different sensors are acquired and synchronized through a data acquisition system at a constant sampling rate of 500 Hz. Finally, the Kalman filter provides the estimation of the four track irregularities.

4.2 Kalman filter

The state vector is composed of the lateral and vertical displacement of both rails from their ideal positions, along with their first and second spatial derivatives. It can be expressed as:

$$\mathbf{x} = \begin{bmatrix} y^{lir} & y^{rir} & y^{lir\prime} & y^{rir\prime} & y^{lir\prime\prime} & y^{rir\prime\prime} & z^{lir} & z^{rir} & z^{lir\prime} & z^{rir\prime} & z^{lir\prime\prime} & z^{rir\prime\prime} \end{bmatrix}^T \tag{15}$$

The measurement vector includes gyroscope signals and the gauge variation measured by the LVDT distance sensor.

$$\mathbf{z}_{meas} = \begin{bmatrix} \omega_x^{gyr} & \omega_y^{gyr} & \omega_z^{gyr} & \xi_{gv}^{meas} \end{bmatrix}^T \tag{16}$$

The Kalman filter is based on two different kind of equations: the system and the measurement equations. The system equation in the discrete form, which relates the state at instant k and k-1 is represented as:

$$\mathbf{x}_k = \mathbf{F}\,\mathbf{x}_{k-1} + \mathbf{v}_k \tag{17}$$

where $\mathbf{F}$ is the state transition matrix, which is given by:

$$\mathbf{F} = \begin{bmatrix} \mathbf{F}_L & 0 \\ 0 & \mathbf{F}_V \end{bmatrix}; \qquad \mathbf{F}_L = \mathbf{F}_V = \begin{bmatrix} 1 & 0 & V\Delta t & 0 & 0 & 0 \\ 0 & 1 & 0 & V\Delta t & 0 & 0 \\ 0 & 0 & 1 & 0 & V\Delta t & 0 \\ 0 & 0 & 0 & 1 & 0 & V\Delta t \\ 0 & 0 & 0 & 0 & 1 & 0 \\ 0 & 0 & 0 & 0 & 0 & 1 \end{bmatrix} \tag{18}$$

The system model is usually referred in literature as *Wiener process acceleration state model* [20]. As can be seen, the state transition matrix $\mathbf{F}$ depends on forward velocity V and the time increment Δt. The term $\mathbf{v}_k$ is the process noise, which can be modelled as zero-mean Gaussian noise with covariance matrix $\mathbf{Q}$.

The measurement process in the discrete form, at instant k, can be expressed through the following equation.

$$\mathbf{z}_k = \mathbf{H}\mathbf{x}_k + \mathbf{G} + \mathbf{w}_k \tag{19}$$

where $\mathbf{H}$ is the measurement transition matrix, and $\mathbf{G}$ is an input matrix. These matrices can be obtained by substituting Eqs. 5-6 for Eqs. 13-14 to obtain:

$$\mathbf{H} = \begin{bmatrix} 0 & 0 & 0 & 0 & 0 & 0 & 0 & 0 & V/2L_r & -V/2L_r & 0 & 0 \\ 0 & 0 & 0 & 0 & 0 & 0 & 0 & 0 & 0 & 0 & -V & 0 \\ 0 & 0 & 0 & 0 & V & 0 & 0 & 0 & 0 & 0 & 0 & 0 \\ 1 & -1 & 0 & 0 & 0 & 0 & 0 & 0 & 0 & 0 & 0 & 0 \end{bmatrix} \tag{20}$$

$$\mathbf{G} = [0\ ,\ 0\ ,\ \rho_h V\ ,\ 0]^T \tag{21}$$

In this case, term $\mathbf{w}_k$ is the measurement noise, which can be modelled as zero-mean Gaussian noise with covariance matrix $\mathbf{R}$. It is important to note that, both process and measurements noises have been modelled as zero-mean Gaussian noise. Since they are due to many random and cumulative sources of error, and because of the central limit theorem, it is common and reasonable to assume that noise errors are Gaussian.

New features of the proposed Kalman filter in comparison with the filter reported previously in [18] include the reduction of required sensors (suppressing the accelerometers) and the elimination of the *virtual sensor* used to avoid the drift in the estimation of irregularities.

5 Experimental setup

This section presents the experimental validation of track irregularities estimation through the use of the methodology proposed in this paper. To do this, the ideal process would be to validate the proposed methodology in a real scenario. However, the difficulty of carrying out experiments on real railroad vehicles and tracks is a major drawback from a research point of view. To solve this problem, the University of Seville's railway research group built a 1:10-scale track facility, which includes a 90-meter-long scaled track and an instrumented scaled vehicle [21]. The subsequent sections will outline the main characteristics of the scaled track facility: scaled track and instrumented axle.

5.1 Experimental scaled track

The experimental campaign was carried out on a 5-inch wide 1:10-scale experimental track installed on the rooftop of the School of Engineering at the University of Seville. The scale track is 90-meter long with a design geometry comprising a combination of tangent sections, transitions, and constant curvature sections, similarly to real scale tracks. The design of the scale track is depicted in Fig. 5. In the figure, the different types of section have been highlighted in different colors. Additionally, the type, length and location of each section have also been included.

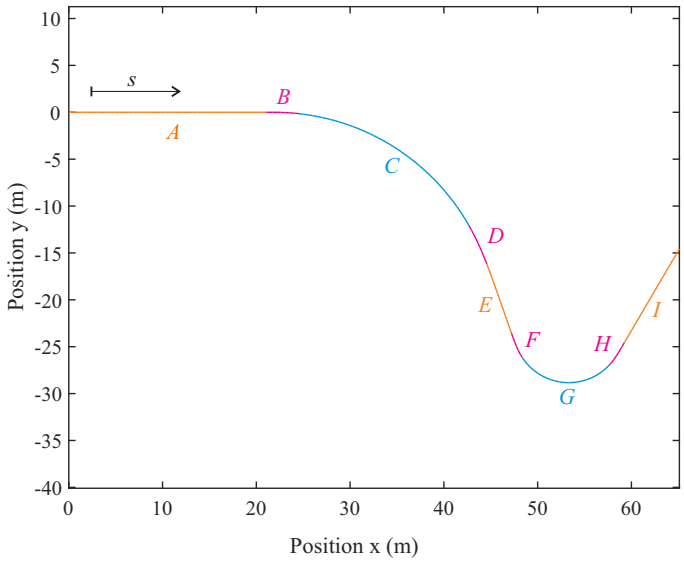

Section	Type	Start	End
A	Tangent	0 m	22 m
B	Transition	22 m	25 m
C	Curve	25 m	51 m
D	Transition	51 m	54 m
E	Tangent	54 m	60 m
F	Transition	60 m	63 m
G	Curve	63 m	75 m
H	Transition	75 m	78 m
I	Tangent	78 m	90 m

Fig. 5. Design of scale track

The track is installed over a set of metallic benches distributed along the rooftop of the building, see Fig. 6 (a). The rails reproduce a scaled version of an real UIC-54 standard profile. Both rails are held using 900 mechanisms that emulate a conventional track sleeper, see Fig. 6 (b). These mechanisms allow the manual insertion of arbitrary track irregularities into the track. Track gauge, angle of cant, and relative height between both rails can be accurately modified by manipulating each mechanism.

(a) (b)

Fig. 6. (a) Scaled track view, (b) detail of adjustable mechanisms

After installation, the scaled track geometry was measured using two different methods [22].

1. *Manual measuring method* (MMM):
   This method is quite slow and tiresome, since it requires the use of a total station together with a distance sensor and an inclinometer to measure the track geometry and its corresponding irregularities in a discrete way. At the end of the experimental measurement, an optimization methodology [22, 23] must be employed to obtain the actual geometry of the track and its corresponding irregularities. The manual procedure is as precise as it is slow: it takes several days to measure the 90 meter long scale track.
2. *Track Recording Vehicle with Total Station* (TRV + TS):

This methodology represents a great advance with respect to the previous one, providing a fast and accurate measurement of the track geometry. It is based on an automated measurement of the track by means of a dedicated vehicle, designed by the authors. The vehicle is equipped with different sensors (an LVDT distance sensor and an inclinometer) to measure the relative position between both rails. Additionally, with the use of an encoder and a total station (with a reflector installed in the vehicle), the geometry of the track centerline can be obtained. Since the accuracy of the total station is only achievable at distances less than 20 meters, the track must be measured section-by-section (three in this case), and a subsequent optimization procedure must be applied to obtain the geometry of the track centerline.

Both methodologies turned out to provide similar results in the measurement of the track centerline and its corresponding irregularities. Consequently, these measurements are considered as the reference in the validation of the irregularity estimation obtained through the methodology proposed here.

5.2 Design of the measuring system

The proposed measuring system is based on previous work reported by [18] where a TRV equipped with an instrumented axle was used. With the aim of configuring a measuring system more easily implemented in a real-world, real-scale scenario, only the instrumented axle, propelled by an independent vehicle, has been used in the present methodology. This propelling vehicle can be any railway vehicle. In this work, the instrumented axle was propelled by a bogie vehicle as shown in Fig. 7. The scale bogie vehicle was mainly designed with physical similarity with respect to a real railroad vehicle [24]. The commitment between the imperative design requirements and the desired dynamic behaviour was essential. In this regards, the length scaling factor was 1/10. Assuming that the scale vehicle nominal angular velocity is that of the full scale vehicle, the forward speed scaling factor is 1/10.

The maximum forward velocity of the propelling vehicle is that which ensures that the instrumented axle is able to properly follow the rail geometry. In the present work, a maximum forward speed of 0.8 m/s (29 Km/h in real scale scenario) has provided very good results. However, this moderate forward speed could be increased by improving the mechanical design of the instrumented axle, which is planned as a future work.

Fig. 7. Instrumented axle and propelling vehicle on the scaled track

The connection between the instrumented axle and the propelling vehicle is made by means of a pulling bar with spherical joints at its ends that decouples the rotation of both elements. The acquisition system together with the Kalman filter algorithm was programmed in the C language and the compiled program was installed on an on-board computer to enable the proposed measuring system to obtain the estimation of track irregularities.

The data acquisition system consists of a Real Time (RT) computer where all the sensors of the vehicle are connected to. The RT controller is a NI MyRIO-1900 (by National Instruments), with a Xilinx Z7010 processor with 2 cores running

at 667 MHz and 256MB of RAM memory. This controller uses a RT Linux version as operating system and has a FPGA included, that manages the different digital and analog ports. In this application, the control of the vehicle and the sensor data acquisition has been programmed in the FPGA module, meanwhile the user interface and the data recording systems run on the RT computer. All the software has been entirely developed using LabView 2018.

As regards the acquisition rate (and consequently, the time step Δt), there are two requirements to be fulfilled. The first requirement is that the measuring system must be able to capture the minimum wavelength irregularity for the forward speed of the vehicle. The second requirement is the precision of the equation discretization: the smaller the time step is, the better precision is achieved. Consequently, with the sampling rate of 500 Hz, both requirements are more than fulfilled for our application and for any real scale application. Finally, it is important to note that the proposed methodology works in real-time, since the time required for calculations is much less than the time step (Δt = 1/500 s).

6 Results and comparison

To validate the proposed estimation procedure, a complete experimental campaign was developed and carried out in the scale track facilities. A total of six experiments were completed involving three different forward speeds (0.5 m/s, 0.65 m/s and 0.8 m/s) with two repetitions for each one. The range of forward speed, which corresponds to [18 - 29 Km/h] in a real scale scenario, is appropriate for a proper measurement of the track geometry by the instrumented axle. For the sake of clarity, only one of the experiments is described here: the experiment with intermediate forward speed V = 0.65 m/s for a total length of 80 m. The results in the estimation are the same in the rest of the experiments, regardless the forward speed and the repetition.

Before using the Kalman filter, the covariance matrices should be estimated. Since the state vector is composed of random and independent variables, the process covariance matrix $\mathbf{Q}$ can be considered as a diagonal matrix with the corresponding process noise variance for each state. In this case, the noise variances for the state corresponding to positions, slopes and curvatures have been taken as: 10^{-20}, 10^{-16} and 10^{-12}, respectively. Since the variables in the measurement vector are random and independent, the measurement covariance matrix $\mathbf{R}$ can be considered as a diagonal matrix with the corresponding noise variance for each measurement. In this case, the noise variances have been estimated from the datasheets of the different sensors: the first three noise variances correspond to gyroscopes (ω_x^{gyr}, ω_y^{gyr} and ω_z^{gyr}), with a value of $(0.0005)^2$ rad^2/s^2, while the fourth noise variance corresponds to the LVDT sensor (ξ_{gv}^{meas}), with a value of $(0.0001)^2$ m^2. These values have been taken based on experience in a previous work [18], where very good results were obtained. Even though is an usual tendency obtaining the noise covariance matrices $\mathbf{Q}$ and $\mathbf{R}$ based on experience, there are several methodologies to estimate both matrices, such as the constrained maximum likelihood (CML) estimation method [25]. This methodology will be used in future works.

6.1 Input data from measurements

The forward speed profile for the selected experiment (V = 0.65 m/s) obtained from the encoder installed in the instrumented axle is presented in Fig. 8. As expected, the forward speed profile is kept constant throughout the whole experiment at the set-point value of V = 0.65 m/s, except at the beginning and end of the ride, where the acceleration and deceleration of the vehicle take place.

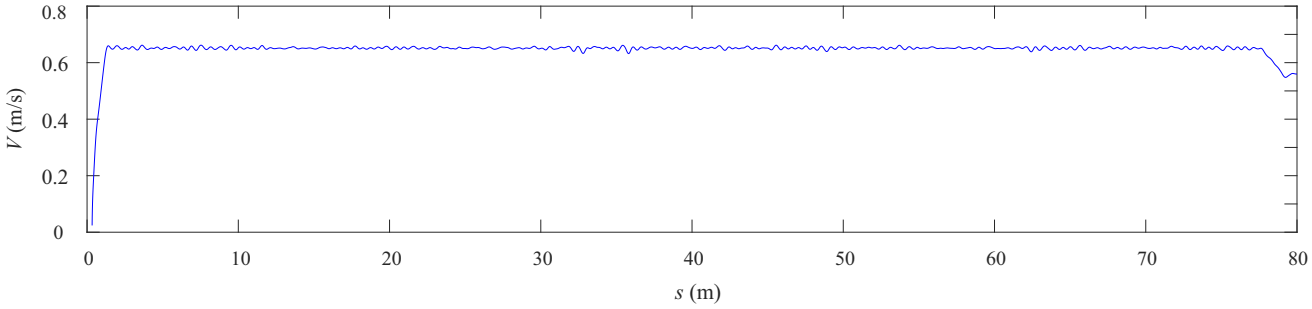

Fig. 8. Forward speed

The experimental data from the sensors installed in the vehicle (gyroscope and LVDT distance sensor) are presented in Figs. 9 and 10 corresponding to vertical and lateral motion respectively.

Some peaks distributed during the experiment can be seen in the sensor data related to vertical motion (see Fig. 9). These peaks correspond to the small gaps between consecutive rail sections. The purpose of these gaps is to absorb the axial

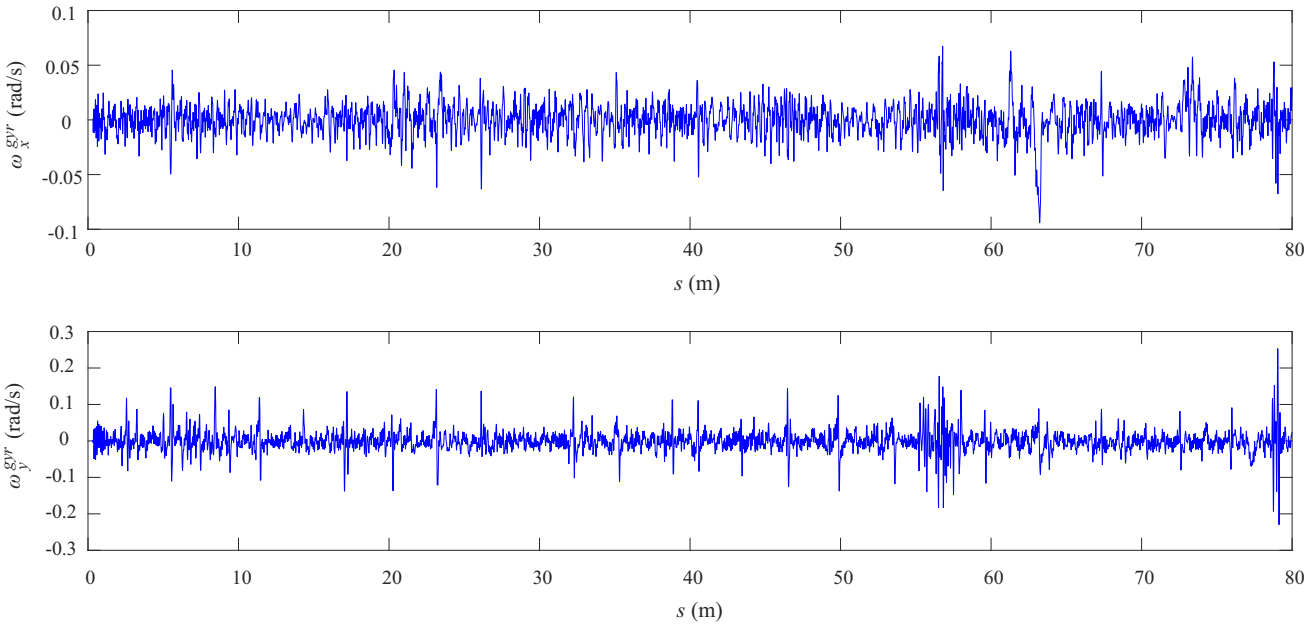

Fig. 9. Input sensor data related to vertical motion: (a) roll-rate, (b) pitch-rate

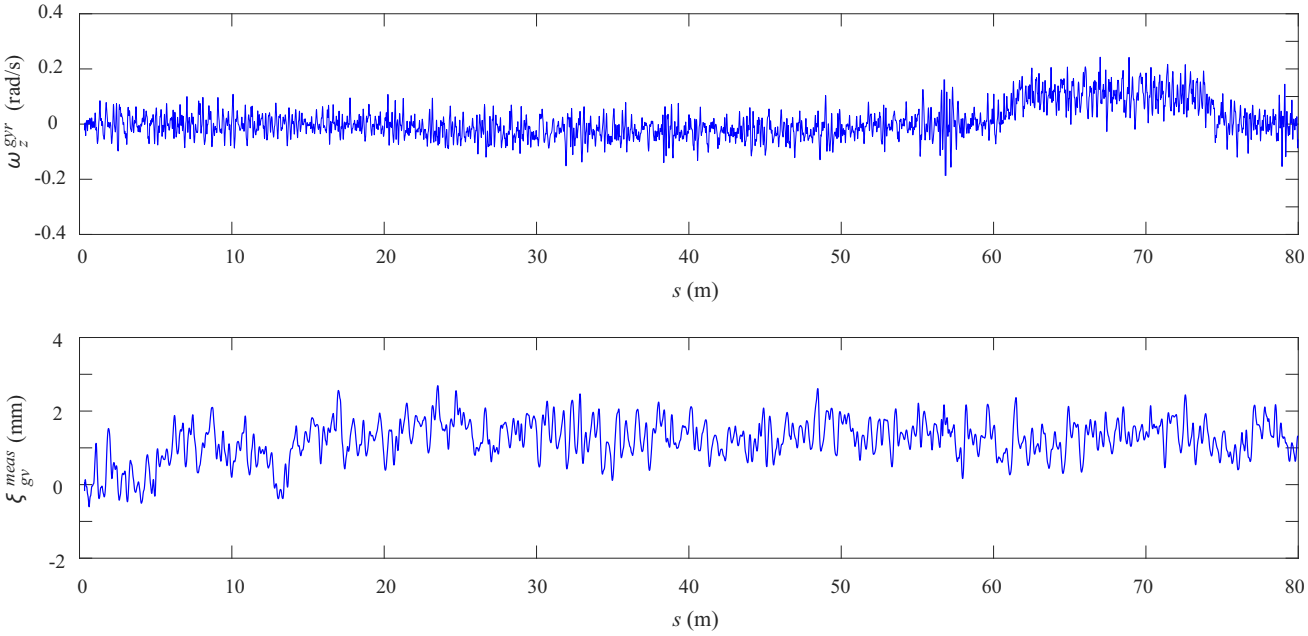

Fig. 10. Input sensor data related to lateral motion: (a) yaw-rate, (b) gauge variation

thermal expansion of the rails due to temperature changes. These peaks in the input data could lead to incorrect estimated irregularities. However, since these peaks correspond to very high frequency content of the input signal, they are easily eliminated at the end of the estimation process when the results are filtered in the range of interest, as will be seen below.

6.2 Estimation of track irregularities

The track irregularities estimated using the proposed methodology were compared to the reference irregularities. As previously commented, the reference geometry of the track was obtained by the experimental methodologies presented in Section 5.1. The estimation of track irregularities obtained by the proposed methodology for the entire track length is shown in Fig. 11. It is important to note that the estimation of track irregularities were obtained in real time. The estimated irregularities were subsequently plotted against the reference irregularities. Before plotting the results, both profiles (”Real” and ”Estimation”) were filtered with a Butterworth bandpass filter in the range of interest according to standards [1]: frequencies corresponding to a wavelength range between 0.3 and 7 m for the 1:10-scaled track (D1-D2 range). The D1-D2

range for a real-world scale track (λ = 3 - 70 m) corresponds to (λ = 0.3 - 7 m) in a 1:10-scaled track.

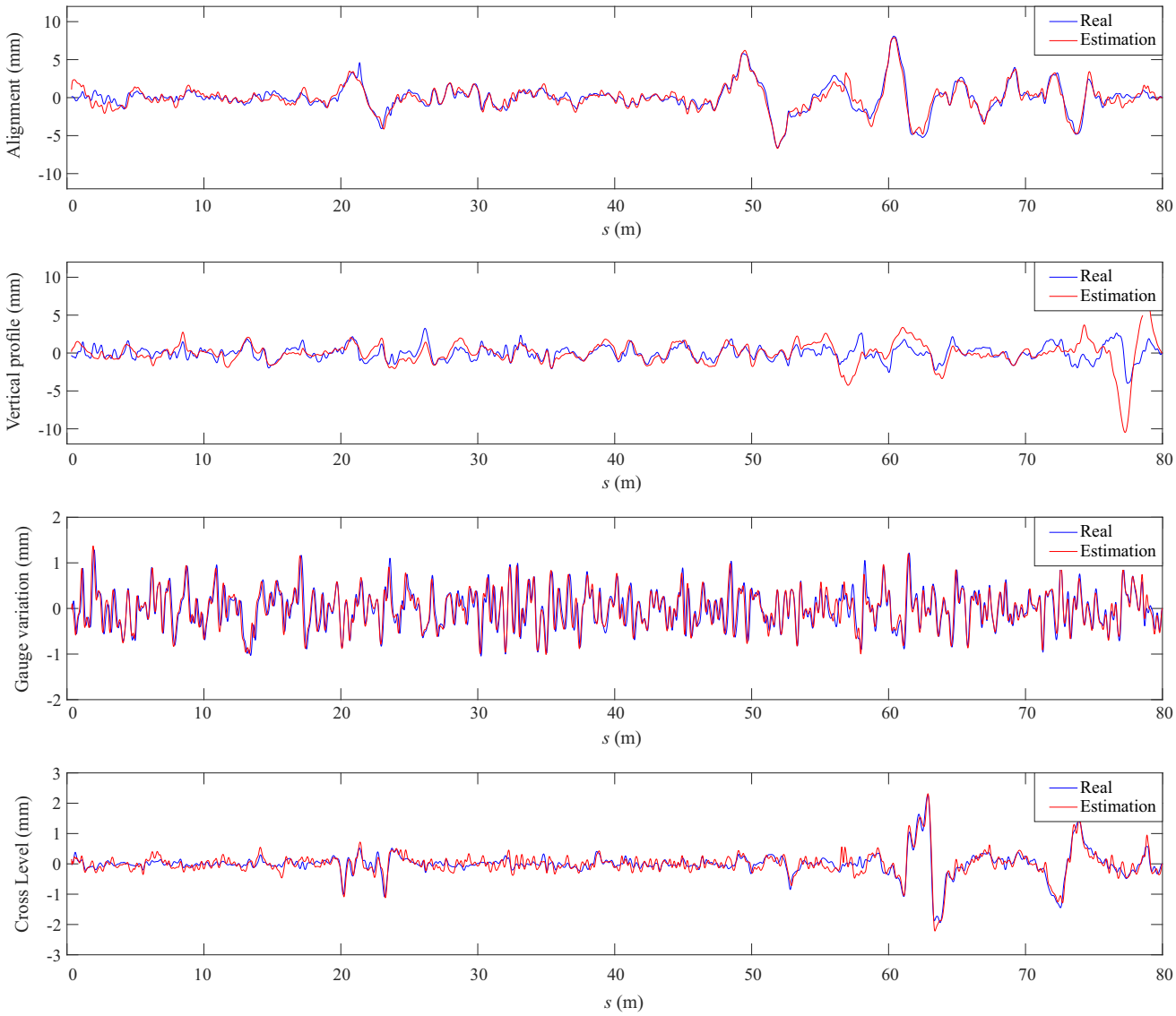

Fig. 11. Estimation of track irregularities, filtered in a D1-D2 range (λ = 0.3 - 7 m)

For deeper analysis, the results of the estimation are presented separately in each wavelength range: D1 range (λ = 0.3 - 2.5 m) in Fig. 12 and D2 range (λ = 2.5 - 7 m) in Fig. 13.

To complete the information and numerically evaluate of the results achieved with the proposed method, the following accuracy index was calculated.

$$J = rms\left(\xi_{est} - \xi_{real}\right) \tag{22}$$

The root mean square value (rms) of the difference between the real and estimated irregularity is used to determine an absolute accuracy index, denoted as J and measured in length units. This accuracy index provides an intuitive and useful measure of the quality of the estimation procedure. Thus, the accuracy index for the different wavelength ranges taken into consideration (whole range, D1 and D2) is presented in Table 1.

In light of the results presented in Fig. 11, good agreement was observed between the estimated and reference track irregularities along the entire length of the scaled track. In general, an accurate estimation of all irregularities is observed in Fig. 11, which can be verified with the accuracy index presented in Table 1. As regards relative irregularities (gauge

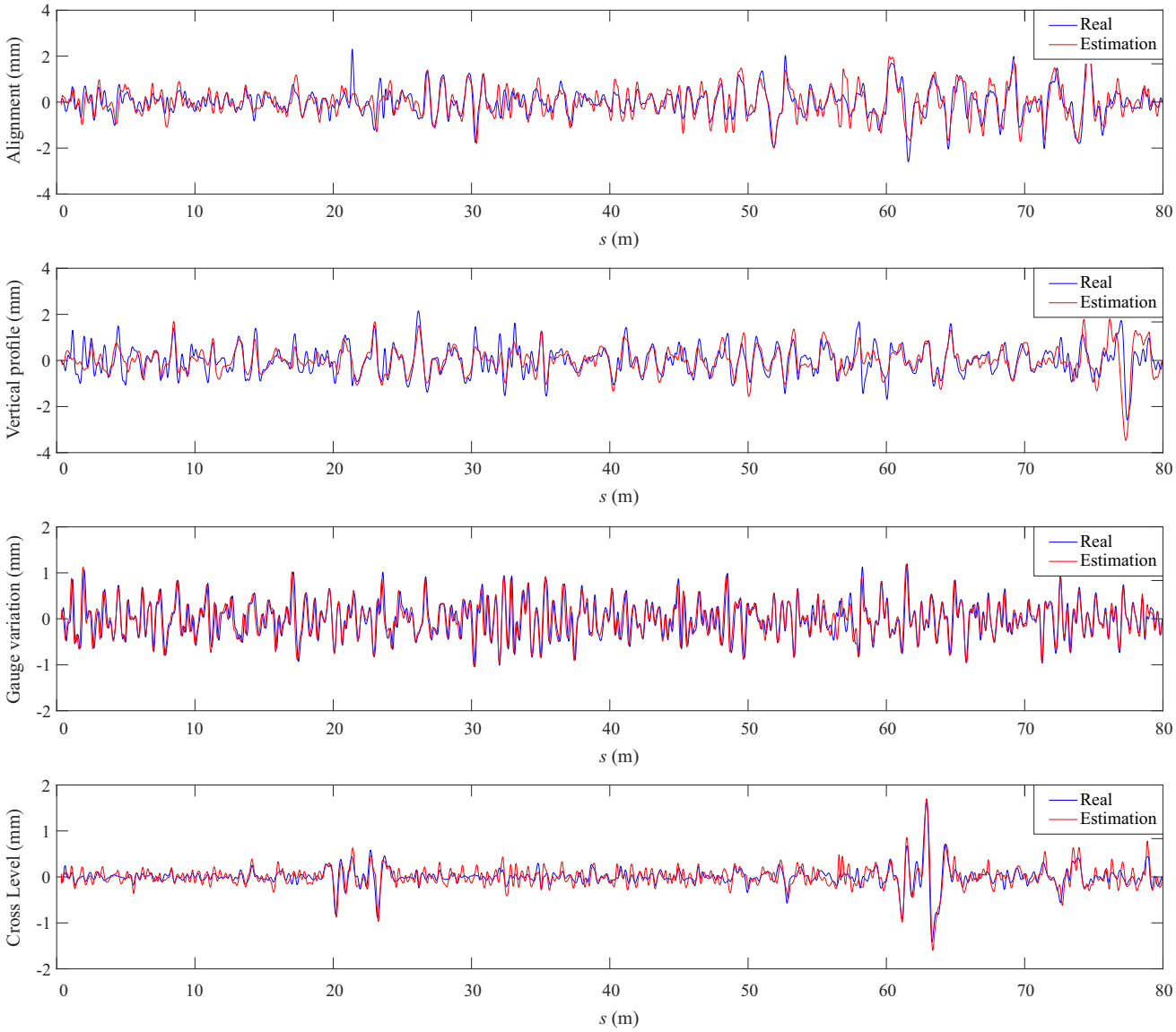

Fig. 12. Estimation of track irregularities, filtered in the D1 range (λ = 0.3 - 2.5 m)

Table 1. Accuracy index, J (in mm), in different wavelength ranges

	D1+D2	D1 range	D2 range
Alignment	0.65	0.37	0.54
Vertical profile	1.53	0.45	1.35
Gauge variation	0.20	0.20	0.03
Cross level	0.15	0.12	0.08

variation and cross level), there is a good agreement, with an accuracy index J lower than 0.20 mm. Regarding the global irregularities, the results are less precise, as expected. Values of J = 0.65 and 1.53 mm were found for alignment and the vertical profile, respectively. The largest level of disagreement was in the estimation of the vertical profile (J = 1.53 mm). As Fig. 11 shows, this disagreement is mainly found in the last transition segment, at s = 75 m.

When analyzing the results in the different wavelength rages (D1 and D2) separately, estimation results show a clear trend: there is good agreement in the D1 range for all irregularities, as observed in Fig. 12, with an error J lower than

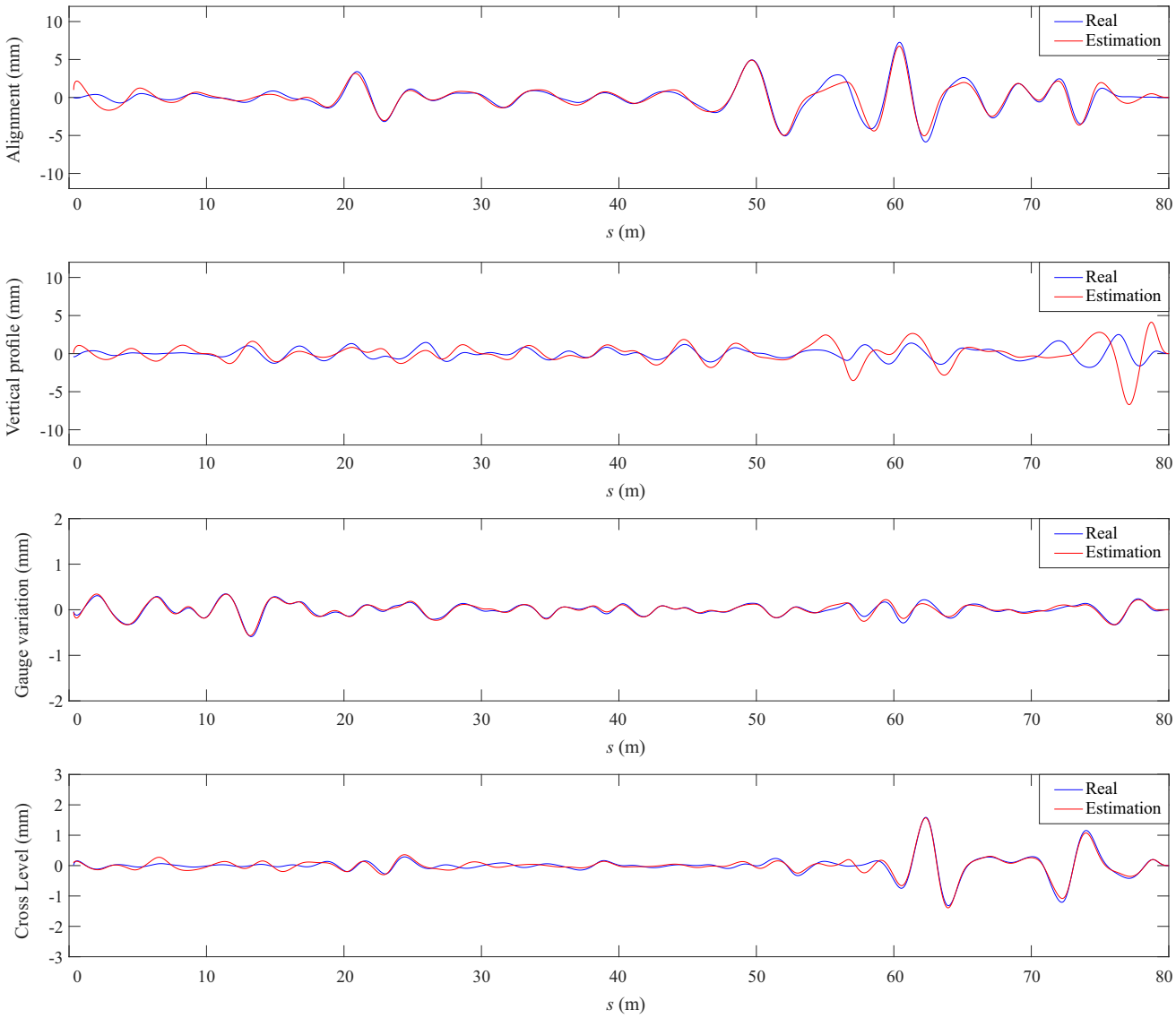

Fig. 13. Estimation of track irregularities, filtered in the D2 range (λ = 2.5 - 7 m)

0.45 mm. Regarding the results in the D2 range, (see Fig. 13), clear disagreement is only observed in the vertical profile estimation in the last transition segment (s = 75 m). This disagreement is reflected in the value of J = 1.35 mm for the D2 range shown in Table 1.

The experimental campaign on the scaled track showed good results in track irregularity estimation, validating the proposed methodology. Especially interesting are the good results in the short wavelength range (D1), which is the most influential one in terms of vehicle dynamic behavior. In fact, it is common practice in the geometry measurement of metropolitan trains to measure irregularities only in the D1 wavelength range.

The highlights of the proposed methodology include different aspects. Firstly, the simplicity of the measurement system, which comprises just an independent device: the instrumented axle. Since the instrumented axle is totally independent of the propelling vehicle, it can be adjusted and calibrated in laboratory. Due to its reduced size, it can be easily transported to any point where is required. And it can be connected to the propelling vehicle through a pulling bar in just few minutes. Consequently, all the above make the measuring system easily implemented in a real-world, real-scale scenario. Secondly, since the Kalman filter algorithm has been programmed in the C language and implemented in the acquisition system, the proposed methodology is real-time capable, making it especially attractive for the railway industry. Finally, the time required for the measuring procedure, which depends on the forward speed of the propelling vehicle, is substantially minimized. A forward speed V of around 25 km/h in a real-scale scenario has been shown to be adequate to obtain good results and quickly. Consequently, due to the fact that the proposed methodology is capable of working on real-time and providing the results immediately after the experiments without any further post-processing, this methodology represents a very interesting and attractive tool for railway track monitoring.

Table 2. Comparison with the previous methodology

		Present method	Previous method
Accuracy index, J	Alignment	0.65 mm	2.75 mm
	Vertical profile	1.53 mm	1.51 mm
	Gauge variation	0.20 mm	0.16 mm
	Cross level	0.15 mm	0.15 mm
Efficiency	Measuring time	123 s	124 s
	Processing time	0 s	20 s

6.3 Comparison with the previous methodology

As previously commented, the present methodology for the estimation of track irregularities is based on a previous methodology presented by the authors in [18], with several improvements. In this section, the improvements related to the Kalman filter algorithm are evaluated. These improvements are: the elimination of the accelerometers from the Kalman filter measurement vector and the implementation of the algorithm in the C language, that makes the proposed procedure real-time capable. Consequently, the present methodology is compared with the previous one, in terms of accuracy and efficiency.

The results of track irregularity estimation of both methods are compared with two different experimental campaigns, with very similar forward speed range. In both cases, three experiments with different forward speed were carried out: V = 0.5 , 0.65 and 0.8 m/s in the present work, and V = 0.5 , 0.7 and 0.9 m/s in the previous work. The results of the comparison are presented in Table 2.

Regarding the accuracy, both methods present very similar values of the accuracy index, J, for all types of irregularities, except alignment, were a notable improvement is achieved with the present methodology: J = 0.65 mm againts J= 2.75 mm. This improvement can be explained by the elimination of accelerometers in the present Kalman filter. Based on these results, it can be concluded that the inclusion of accelerometers did not provide useful information to the Kalman filter and, in the case of alignment, the lateral accelerometer was a source of errors in the estimation method. It is important to note that alignment is the most difficult irregularity to detect. Furthermore, alignment is the most influential irregularity in the dynamic behaviour of the vehicle from both points of view: ride comfort and safety.

Regarding efficiency, the experiment with intermediate forward speed has been analyzed in both cases: V = 0.65 m/s for the present method and V = 0.7 m/s for the previous one. As expected, the time dedicated to the measurement process is similar, since it only depends on the forward speed of the vehicle. However, the main improvement of the present methodology is the processing time that, due to its real-time capability, is reduced to zero. Even though this improvement does not seem to be a great achievement (the processing time of the previous method was only 20 s), the reduction of the processing time can be significant in a real scale scenario, where a large number of kilometers of tracks are measured at one time.

Finally, in light of the results of the comparison, it can be concluded that the present Kalman filter model represents a significant improvement compared to the previous model, in terms of accuracy and efficiency.

7 Summary and conclusions

Based on the previous work by the authors, a new modified methodology for measuring track irregularities has been developed in the present work, with the following improvements. Firstly, instead of using a complete Track recording vehicle, this methodology was developed to be used on an independent and compact measuring system: an instrumented axle that can be propelled by any railway vehicle. From the practical point of view, this represents a significant improvement, since the preparation time of the measurement system is significantly reduced before the measurement process, taking just few minutes to connect the instrumented axle to the propelling vehicle before the track measurement process. Secondly, the proposed methodology is based on an improved Kalman filter, that makes use of a limited set of low-cost sensors: a 3D gyroscope, a Linear Variable Differential Transformer (LVDT) distance sensor, and an encoder. Accelerometers are no longer needed in the present methodology, which represent a major improvement, due to the inherent difficulty of using accelerometers with such a noisy signals. Thirdly, the Kalman filter algorithm was programmed in the C language and implemented in the acquisition system, making the proposed procedure real-time capable. This improvement enables the measurement system to provide a direct measurement of track irregularities in real time, without any type of subsequent post-processing. As regard the modifications in the Kalman filter algorithm (elimination of the acceleromenters from the set of sensors and the implementation of the algorithm in the C language), notable improvements have been achieved in the performance of the present methodology, in terms of accuracy and efficiency. First, the accuracy index J in the present methodology is similar

to the previous method for all types of irregularities, except alignment, where a notable improvement has been achieved. Second, the efficiency of the methodology has also improved, reducing the processing time to zero.

In conclusion, the proposed measuring system represents a final product that should be attractive to the railway industry. Since the instrumented axle is an independent system that can be propelled by any railway vehicle, it is easily implemented in a real-world, real-scale scenario.

The proposed methodology was validated by carrying out an experimental campaign on a 1:10-scale track facility at the University of Seville. The instrumented axle enabled the measurement of 80 meters of the scaled track at an operational velocity of $V = 0.65$ m/s in only two minutes. The track irregularity estimate results were compared against a reference measurement. Good agreement was demonstrated with errors lower than 0.45 mm in the short wavelength range D1, which is the most influential in the dynamic behavior of the vehicle.

Acknowledgements

This research was supported by the Spanish *Ministerio de Ciencia e Innovacion*, under the program "Proyectos I+D+I?2020" with project reference PID2020-117614RB-I00. It was also supported by the Spanish *Department of Economy, Science, Enterprise and University of the Andalusian Regional Government*, under the PAIDI 2020 program with project reference P18-RT-1772. The support is gratefully acknowledged.

References

[1] CEN European Commitee for Standarization, 2009. Railway Applications - Track - Track Geometry Quality - IS EN 13848-5.

[2] Sanchez, A., Bravo, J. L., and Gonzalez, A., 2017. "Estimating the accuracy of track-surveying trolley measurements for railway maintenance planning". *Journal of Surveying Engineering,* **143**(1).

[3] Akpinar, B., and Gulal, E., 2012. "Multisensor railway track geometry surveying system". *IEEE Transactions on Instrumentation and Measurement,* **61**(1), pp. 190–197.

[4] Grassie, S. L., 1996. "Measurement of railhead longitudinal profiles: a comparison of different techniques". *Wear,* **191**(1), pp. 245–251. 4th International Conference on Contact Mechanics and Wear of Rail-Wheel Systems.

[5] Baier, M., Rulka, W., and Abel, D., 2009. "Model based measurement of railway track irregularities". *IFAC Proceedings Volumes,* **42**(15), pp. 257–262. 12th IFAC Symposium on Control in Transportation Systems.

[6] Weston, P., Roberts, C., Yeo, G., and Stewart, E., 2015. "Perspectives on railway track geometry condition monitoring from in-service railway vehicles". *Vehicle System Dynamics,* **53**, pp. 1063–1091.

[7] Ward, C., Weston, P., Stewart, E., Li, H., Goodall, R., Roberts, C., Mei, T., Charles, G., and Dixon, R., 2011. "Condition monitoring opportunities using vehicle-based sensors". *Proceedings of the Institution of Mechanical Engineers, Part F: Journal of Rail and Rapid Transit,* **225**(2), p. 202 – 218.

[8] Molodova, M., Li, Z., and Dollevoet, R., 2011. "Axle box acceleration: Measurement and simulation for detection of short track defects". *Wear,* **271**, 05, pp. 349–356.

[9] OBrien, E. J., Quirke, P., Bowe, C., and Cantero, D., 2018. "Determination of railway track longitudinal profile using measured inertial response of an in-service railway vehicle". *Structural Health Monitoring,* **17**(6), pp. 1425–1440.

[10] La Paglia, I., Carnevale, M., Corradi, R., Di Gialleonardo, E., Facchinetti, A., and Lisi, S., 2023. "Condition monitoring of vertical track alignment by bogie acceleration measurements on commercial high-speed vehicles". *Mechanical Systems and Signal Processing,* **186**, p. 109869.

[11] Weston, P., Ling, C. S., Roberts, C., Goodman, C. J., Li, P., and Goodall, R. M., 2007. "Monitoring vertical track irregularity from in-service railway vehicles". *Proceedings of the Institution of Mechanical Engineers, Part F: Journal of Rail and Rapid Transit,* **221**(1), pp. 75–88.

[12] Weston, P., Ling, C. S., Goodman, C. J., Roberts, C., Li, P., and Goodall, R. M., 2007. "Monitoring lateral track irregularity from in-service railway vehicles". *Proceedings of the Institution of Mechanical Engineers, Part F: Journal of Rail and Rapid Transit,* **221**(1), pp. 89–100.

[13] Tsunashima, H., Naganuma, Y., and Kobayashi, T., 2014. "Track geometry estimation from car-body vibration". *Vehicle System Dynamics,* **52**(sup1), pp. 207–219.

[14] Seok Lee, J., Choi, S., Kim, S.-S., Park, C., and Guk Kim, Y., 2012. "A mixed filtering approach for track condition monitoring using accelerometers on the axle box and bogie". *IEEE T. Instrumentation and Measurement,* **61**, 03, pp. 749–758.

[15] De Rosa, A., Alfi, S., and Bruni, S., 2019. "Estimation of lateral and cross alignment in a railway track based on vehicle dynamics measurements". *Mechanical Systems and Signal Processing,* **116**, pp. 606 – 623.

[16] Muñoz, S., Ros, J., Urda, P., and Escalona, J. L., 2021. "Estimation of lateral track irregularity using a Kalman filter. experimental validation". *Journal of Sound and Vibration,* **504**, p. 116122.

[17] Liao, Y., Han, L., Wang, H., and Zhang, H., 2022. "Prediction models for railway track geometry degradation using machine learning methods: A review". *Sensors,* **22**(19).

[18] Muñoz, S., Urda, P., and Escalona, J. L., 2022. "Experimental measurement of track irregularities using a scaled track recording vehicle and Kalman filtering techniques". *Mechanical Systems and Signal Processing,* **169**, p. 108625.

[19] Escalona, J. L., Urda, P., and Muñoz, S., 2021. "A track geometry measuring system based on multibody kinematics, inertial sensors and computer vision". *Sensors,* **21**(3).

[20] Brown, R., and Hwang, P., 2012. *Introduction to random signals and applied Kalman filtering with Matlab exercises*. Wiley, New York.

[21] Urda, P., Muñoz, S., Aceituno, J. F., and Escalona, J. L., 2020. "Application and experimental validation of a multibody model with weakly coupled lateral and vertical dynamics to a scaled railway vehicle". *Sensors,* **20**(13).

[22] Urda, P., Aceituno, J. F., Muñoz, S., and Escalona, J. L., 2021. "Measurement of railroad track irregularities using an automated recording vehicle". *Measurement,* **183**, p. 109765.

[23] Aceituno, J. F., Chamorro, R., Muñoz, S., and Escalona, J. L., 2019. "An alternative procedure to measure railroad track irregularities. application to a scaled track". *Measurement,* **137**, pp. 417–427.

[24] Aceituno, J. F., Chamorro, R., García-Vallejo, D., and Escalona, J. L., 2017. "On the design of a scaled railroad vehicle for the validation of computational models". *Mechanism and Machine Theory,* **115**, pp. 60–76.

[25] González-Carbajal, J., Urda, P., Muñoz, S., and Escalona, J. L., 2023. "Estimation of the trajectory and attitude of railway vehicles using inertial sensors with application to track geometry measurement". *Vehicle System Dynamics,* **0**(0), pp. 1–27.